J Nanopart Res (2013) 15:1923
DOI 10.1007/s11051-013-1923-8

RESEARCH PAPER

New hybrid titanate elongated nanostructures through organic dye molecules sensitization

V. C. Ferreira · O. C. Monteiro

Received: 30 January 2013 / Accepted: 8 August 2013 / Published online: 21 August 2013

Abstract This study reports on a novel chemical route to synthesize new elongated titanates nanostructured hybrid materials by the combination of titanate nanofibers (TNFs) with organic dye molecules. The influence of the sodium/proton replacement on the adsorption and intercalation characteristics of the TNFs materials was analysed. Depending on the sodium/proton content, materials with surface areas in the 21.08–38.90 m^2/g range were obtained. Due to their molecule size and shape, and anticipating their intercalation between the TiO_6 layers, the cationic molecules chosen for this study were thionine, methylene blue, crystal violet and rhodamine 6G. The sample with the highest sodium content was the best material on up taking dyes from aqueous media. The amount of the immobilized dyes was higher than the one predictable for the formation of a monolayer in an adsorption process. The intercalation of thionine, methylene blue and crystal violet between the TiO_6 layers was accomplished. The characterisation results obtained by adsorption, XRD and FTIR are in agreement with the production of these new hybrid structures, with the organic molecules located within the TiO_6 layers. The results also demonstrate that only the thionine was incorporated in the protonated titanate structure, due to the smaller distance between the layers. The optical characterisation of the prepared materials by DRS also indicates that intercalated and adsorbed dyes have strong influence on the optical properties of the new hybrid materials prepared.

Keywords Elongated titanate nanostructures · Organic dyes · Dye adsorption · Organic molecules intercalation · Nano-hybrid materials

Introduction

Although the titanium oxide (TiO_2) or titania (*anatase* and *rutile*) being the titanium compound most commonly used in several applications, including photocatalysis (Luis et al. 2011), the nanostructured titanates, either protonated or doped with sodium ions, with general formula $Na_{2-x}H_xTi_3O_7{\cdot}nH_2O$, with $0 \leq x \leq 2$ have gained considerable research interest (Bavykin et al. 2009; Zhang et al. 2005).

The generalized chemical formula of the elongated sodium titanates is assumed to be $Na_2Ti_3O_7$, while the protonated titanates is thought to be $H_2Ti_nO_{(2n+1)}{\cdot}xH_2O$. The titanate nanotubular structures have a characteristic multilayered arrangement consisting of edge- and corner-sharing TiO_6 octahedra, having an arrangement

Electronic supplementary material The online version of this article (doi:10.1007/s11051-013-1923-8) contains supplementary material, which is available to authorized users.

V. C. Ferreira · O. C. Monteiro (✉)
Department of Chemistry and Biochemistry and CQB, Faculty of Sciences, University of Lisbon, Campo Grande, 1749-016 Lisbon, Portugal
e-mail: ocmonteiro@fc.ul.pt

forming layers with negative electrical charges between them. This arrangement makes these nanotubes highly efficient for ion-exchange processes and if submitted to weak acid conditions, the sodium ions can be partial or completely replaced by protons. The crystalline structures of layered $Na_2Ti_3O_7$ and $H_2Ti_3O_7$ are similar. The main difference between these two structures is the position of the interlayer cations, H^+ and Na^+: the H^+ ions are adsorbed on the titanate layers, but the Na^+ ions are free between the layers (Zhang et al. 2005).

Alkali metals (Viana et al. 2011), metals, alkylammonium molecules and dyes have been used to replace the sodium ions in the TNFs structure. The diffusion of alkali metals (e.g. Li^+, Na^+, K^+ and Cs^+) probably occurs along the nanotubes length (Bavykin and Walsh 2007), hence depending on the nanotubes size.

The typical interlayer distance of titanates is about 0.74–0.9 nm (Bavykin et al. 2006; Ma et al. 2005), which is higher than the size of most alkali metal cations. Consequently no change in the interlayer spacing would be expected upon cation exchange, as observed for Li^+, Na^+, K^+, Rb^+ and Cs^+, up to $\sim$70 % substitution (Ma et al. 2005). However, XRD analysis have shown expansion of the titanate layers (ca. 0.3 nm) and no selectivity was found between Li^+, Na^+, K^+ and Cs^+ (Bavykin and Walsh 2007). Moreover, the simple exchange of sodium by protons, upon acid treatment, is expected to affect this parameter as indicated by the *d*(200) diffraction peak in the XRD pattern for the $H_2Ti_3O_7$ and $Na_2Ti_3O_7$. In accordance with this, an increase of ca. 0.9 and 1.28 nm was detected by XRD after intercalation of alkylammonium and cyanide dye molecules, respectively (Miyamoto et al. 2004).

The typical values for the titanate nanotubes' surface area are 200–300 m^2/g and for other elongated nano titanates 20–50 m^2/g (Bavykin et al. 2009; Kasuga et al. 1998). These materials have a band gap energy close to that of TiO_2 nanocrystalline *anatase* ($\sim$3.2 eV) (Riss et al. 2007), and they present high facility to be doped with different cationic ions, e.g. Li^+, Cs^+, Na^+, K^+ and dyes (Bavykin and Walsh 2007; Miyamoto et al. 2004; Xiao et al. 2008). This TNFs' ion-exchangeable ability makes them attractive for new photosensitive, adsorbing, solar cells and catalytic materials platforms development (Bavykin et al. 2006; Xiao et al. 2008). Additionally, TiO_2-based nanotubular structures are known to be biocompatible and nontoxic to cells and have been studied to immobilize, transport and delivery of proteins and related biological entities. Recent studies have shown that myoglobin and cytochrome *c* can be successfully immobilized on hydrogen titanate (Ray et al. 2011).

The combination of inorganic host lattices with organics, not only by intercalation but also following the grafting and sol–gel procedures, has been a promising synthesis methodology for designed organic–inorganic materials provided with multifunctional performance for future technological applications (Matsuo and Konishi 2012). On the other hand, recently has been reported that after sodium titanate nanotubes and organic acids interaction, at high temperatures, the nanoparticles exhibited changes in their composition, crystalline structure and morphology, due to a $Na^+ \rightarrow H^+$ ion exchange reaction. At room temperature, the nanotubes stability depends on the nature of the acid used. For instance for benzoic acid, the morphology and structure of the nanoparticles were maintained, but their chemical composition was different (Rodrigues et al. 2010).

Several works have been published related with this issue including co-sensitization with semiconductor nanoparticles and zinc porphyrin (Li et al. 2012) or phthalocyanin-sensitization (Cheng et al. 2010).

A large group of heterocyclic poly-aromatic compounds, such as methylene blue (MB) and rhodamine 6G (R6G), have been intercalated through ion-exchange processes. The intercalation of organic dyes into V205 gels to produce nanocomposite materials of potential interest as photoactive or electro-photoactive systems was one of the first reports related with this subject (Ackermans et al. 1996). The most interesting feature in the visible spectra of cationic dyes such as MB when intercalated, e.g. in clays, is the metachromasy effect. This effect consists in a decrease of the absorption intensity bands assigned to isolated species (dye monomers), accompanied by an increase in the intensity bands at higher energies assigned to the formation of dyes aggregates. This effect that has been spectroscopically deduced for several adsorbed cationic dyes is related to a self-aggregation process in order to give dimers, trimers and higher aggregates. Such aggregates can play an important role as photosensitizers; since, they can transfer triplet energy to the monomer form of the dye, which can serve as an active participant in the energy conversion process.

In the present work, different $Na_{2-x}H_xTi_3O_7{\cdot}nH_2O$ nanocrystalline elongated particles were synthesized and their interaction with the cationic organic dyes, mainly thionine (Th), methylene blue (MB) and crystal violet (CV), was studied. The results demonstrate that the dye immobilization ability was dependent on the samples sodium-content and on the dyes properties. Considering the very high amounts of dye immobilized in the NaTNF samples, the dyes intercalation possibility was analysed. The obtained results evidence the occurrence of some of the organic molecules intercalation, between the TiO_6 layers. The optical properties of the hybrid materials prepared were also analysed and discussed based on the dyes intercalation phenomenon.

Experimental

All reagents were of analytical grade (Aldrich and Fluka) and were used as received without further purification. The solutions were prepared using bi-distillated water.

Materials and methods

TNFs synthesis

The TNFs precursor was prepared using a procedure previously reported (Nunes et al. 2008). A titanium trichloride solution (10 wt% in 20–30 wt% HCl) was diluted in a ratio of 1:2 in a standard HCl solution (37 %). A 4 M ammonia aqueous solution was added drop-wise to this violet dark solution, under vigorous stirring, until complete precipitation of a white solid (TNFs precursor). The resulting suspension was kept overnight at room temperature and then filtered and washed several times with deionised water.

The TNFs samples were obtained by a hydrothermal method using a suspension of $\sim$6 g of this precursor, in ca. 60 ml of NaOH 10 M aqueous solution (Ylhainen et al. 2012). The samples were prepared at 200 °C using an autoclave dwell time of 12 h. After cooling, the suspensions were filtrated and the white solid was washed systematically with water: the sample was dispersed in $\sim$150 mL of water and magnetically stirred for 1 h. Then, the suspension was filtered and the *pH* of the filtrate measured for reference. This procedure was repeated until filtrate solution reached $pH = 7$. The white solid was afterwards dried and stored. The wet-solid NaTNF, obtained from 6 g of precursor, was also used to prepare a protonated sample (HTNF) by dispersing and stirring it in 100 mL of a HNO_3 0.1 M aqueous solution (*pH* 1.2) for 1 h. Next, the solid was washed with water until a filtrate with $pH = 5$ was obtained. This solid (HTNF) was then dried and stored.

Dye adsorption

The adsorption studies were carried out using a dye-TNFs aqueous suspension (1 g L^{-1}) under stirring for 2 h in dark conditions. After centrifugation, the dyes concentrations were estimated by measuring the absorbance at each dye chromophoric peak. When different dyes concentrations (5–250 mg L^{-1}) were used, the TNFs samples were label as dye(I)-TNFs, dye(II)-TNFs and dye(S)-TNFs, being the dye concentration dye(I) < dye(II) < dye(S); the dye(S)-TNFs corresponds to the dye saturation situation.

In order to better understand the surface phenomena involved in the adsorption process, different organic dyes, with distinct molecule dimensions, were used. The following dyes were tested: thionine (Th), crystal violet (CV), rhodamine 6G (R6G) and methylene blue (MB). The solutions' *pH* was 5.7 for Th, 5.5 for CV and MB and 5.4 for the R6G solution.

Characterisation

X-ray powder diffraction was performed using a Philips X-ray diffractometer (PW 1730) with automatic data acquisition (APD Philips v3.6B), using Cu K_α radiation ($\lambda = 0.15406$ nm) and working at 40 kV/30 mA. The diffraction patterns were collected in the range $2\theta = 7°$–$60°$ with a 0.02° step size and an acquisition time of 2.0 s/step. Optical characterisation of the samples was carried out by UV–Vis diffuse reflectance using a Shimadzu UV-2600PC spectrophotometer. Diffuse reflectance spectra (DRS) were recorded in the wavelength range of 220–1,400 nm using an ISR 2600plus integration sphere. Transmission electron microscopy (TEM) and high resolution transmission electron microscopy (HRTEM) were carried out using a JEOL 200CX microscope operating at 200 kV. Specific surface areas were obtained by the BET method, from nitrogen (Air Liquide, 99.999 %) adsorption data at −196 °C, using a volumetric

apparatus from Quantachrome mod NOVA 2200e. The samples, weighing between 40 and 60 mg, were previously degassed for 2.5 h at 150 °C at a pressure lower than 0.133 Pa. Zeta potentials of the samples were measured with an electrophoresis instrument (Model ELS-8000, Otsuka, Japan). An electrolyte solution (1 mM KCl) was used to keep the ionic strength constant, while the *pH* value was varied by adding 0.01 N KOH or HCl into the solution. The *pH* of the suspension was taken as the isoelectric point (IEP) at which the zeta potential was zero.

Results and discussion

NaTNF and HTNF characterisation

The NaTNF and HTNF samples prepared at 200 °C during 12 h were analysed by XRD and the results are presented in Fig. 1. The XRD patterns are in agreement with the existence of a $Na_xH_{2-x}Ti_3O_7$ titanate layered crystalline structure in both samples. The peaks at 24.5°, 28.6° and 48.6° are characteristic of tri-titanate 1D nanomaterials (Wong et al. 2011). The diffraction peak at $2\theta \sim 10^\circ$ is related with the interlayer distance between the TiO_6 layers and can vary depending on the amount, size and nature of the intercalated ion/species. When the reference *pH* decreases, from 7 to 5 (NaTNF and HTNF samples, respectively), the peaks at $\sim 10^\circ$ shifts to higher 2θ values. In addition to this shift, a broadening of these peaks was also observed with the decrease of the reference *pH*. These structural features are related with different sodium contents in the samples, and are indicative of a $Na^+ \rightarrow H^+$ substitution process in the interlayer region (Wong et al. 2011). The decrease in the interlayer dimension is also supported by the release of several water molecules that were surrounding the Na^+ ions, during the ion-exchange process (Bavykin and Walsh 2010). Moreover, the decrease of a characteristic $Na_2Ti_3O_7$ peak intensity (e.g. $2\theta = 25.7^\circ$) also indicates the sodium/proton replacement in the crystalline structure. The XRD and EDS analyses (not shown) are consistent with a gradual sodium/proton replacement that increases with the number of washing steps. Furthermore, the results obtained for the HTNF sample agree with a total sodium substitution.

The NaTNF and HTNF samples were analysed by TEM and elongated nanofiber morphology was observed for the two samples (Fig. 1—inset). The surface areas were measured using the BET methodology and values of 21.08 and 38.90 m^2/g were obtained for the NaTNF and HTNF samples, respectively. The higher value obtained for the HTNF surface area is in agreement with previous reported works (Wong et al. 2011) and it is related with the fact that the removal of the sodium ions turns the interlayer space more accessible for the N_2 molecules during the BET measurements. After total sodium replacement, the material (HTNF) displays a higher surface area without modifying its external morphology.

UV–Vis photo-response

The optical characterisation of the samples was performed by measuring their diffuse reflectance (R) spectra at room temperature. R is correlated with the absorption Kubelka–Munk function, F_{KM}, by the relation $F_{KM}(R) = (1 - R)^2/2R$, being F_{KM} proportional to the absorption coefficient. Figure 2 shows the F_{KM} absorption spectra for both samples. A slight redshift in the optical absorption band edge can be observed for the HTNF sample when compared with the NaTNF. The optical band gap energies of the two samples were calculated by plotting the function $f_{KM} = (F_{KM}\, h\upsilon)^{0.5}$ versus energy (Tauc plot), where h stands for the Planck constant and υ for the frequency. The linear part of the curve was extrapolated to $f_{KM} = 0$ to get the indirect band gap energy for each material (Diamandescu et al. 2008). The estimated E_g values were 3.54 eV for NaTNF and 3.30 eV for the HTNF sample, and are in accordance with previously published ones (Bem et al. 2012).

Point of zero charge

Considering the influence of the surface charge in adsorption processes, the point of zero charge (p.z.c.) of the TNFs samples was evaluated. The *pH* values at which the surface carries no net charge (p.z.c.) were 3.4 and 4.1 for the NaTNF and HTNF samples, respectively. These results are in agreement with reported values for similar titanate nanotubular structures (Bem et al. 2012). The lower p.z.c. value obtained for NaTNF agrees with the

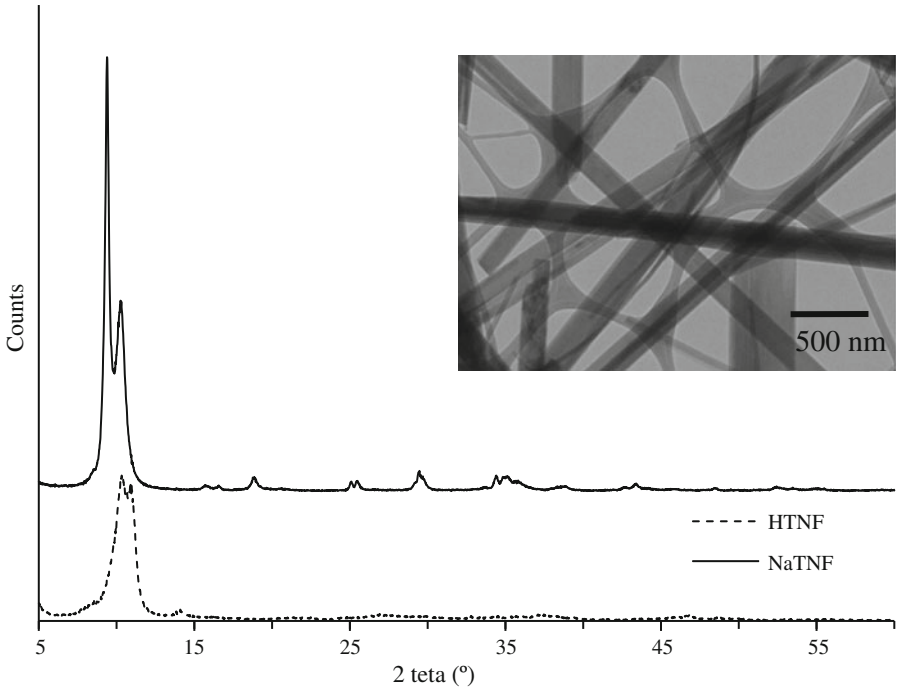

Fig. 1 XRD pattern of the NaTNF and HNT sample; *inset* TEM micrograph of the NaTNF sample

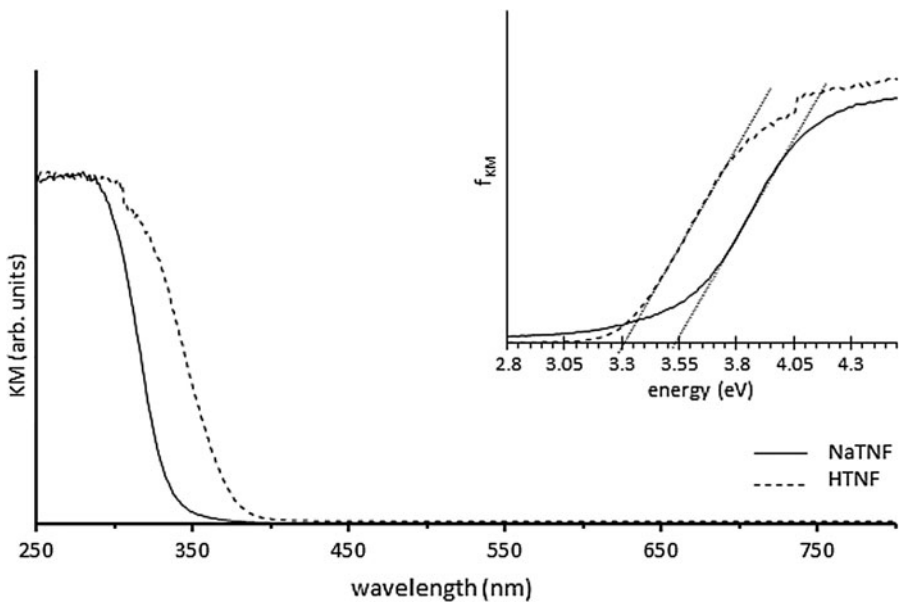

Fig. 2 Absorption spectra of the NaTNF and HTNF samples; *inset* Tauc plots for the TNFs samples synthesized. The optical band gap energies were estimated by extrapolating the linear portion of the curve to zero absorption

existence of some ion-exchange ability for this sample, since it has Na^+ ions remaining in the structure that can be exchanged by cationic species. The shift observed in the p.z.c. value for the HTNF sample, when compared with the NaTNF, is indicative of its higher acidic character.

Dye uptake

Since titanate nanotubular materials (TNFs) have been suggested as adsorbents for cationic species, the prepared samples capability to hold up organic dyes from aqueous solutions was investigated. Aiming to

investigate the influence of the dye molecule size on the TNFs adsorption ability, and considering the p.z.c. of the samples, the organic molecules selected for this study were thionine (Th), methylene blue (MB), crystal violet (CV) and rhodamine 6G (R6G). The chemical structures of these molecules are shown in Fig. 3. Their protonation equilibrium constants are *ca.* −1 for Th (Tchinsoann and Hester 1984), 0.8 for CV (Cui et al. 1995) and <0.5 for MB (Cenens et al. 1988). The pKa value reported for R6G is considerably superior; values between 6.3 and 7.5 have been reported (Khurana et al. 2009). This value, together with the p.z.c. of the TNFs samples, anticipates a R6G lower ability for being adsorbed in the NaTNF and HTNF surfaces.

The amount of the dyes removed after 2 h of stirring was calculated from each solution absorbance and the data, in mg of dye per g of TNFs, is present in Table 1. The NaTNF removal ability for all the dyes was higher than the one calculated for the HTNF sample. Th, the smallest dye molecule and the one with the lowest pKa, had the highest removal level: 126.39 and 9.99 mg g^{-1}, using NaTNF and HTNF, respectively. As expected, considering the NaTNF and HTNF p.z.c. values and the R6G protonation equilibrium constant, the adsorption of this dye was insignificant on both surfaces.

After a careful joined analysis of the *pH* of the dyes' solutions (~5.5), the pKa of the used dyes (*ca.* −1 for Th, 0.8 for CV and 0.5 for MB) and, the p.z.c. of each material (3.4 and 4.1 for the NaTNF and HTNF samples) it is possible to conclude that the differences observed in the uptake capacity of the sodium and protonated TNF forms cannot be attributed to differences in the local *pH* near the surface and a consequent dye's protonation. Actually, and considering the values analysed, the occurrence of the dye's protonation is not expected, even in a reduced extension.

The size of the organic dyes molecules, that adsorb on the NaTNF and HTNF surfaces, increases in the order Th < MB < CV. The area occupied by them in the surface depends on the orientation of the adsorbed molecules (see Electronic Supplementary Material, Fig S1). It can be assumed that the cationic species are adsorbed on the surface through electrostatic interactions and therefore oriented perpendicularly with the positive charge towards the TNFs surface, resulting in an area occupied per molecule of about 0.12, 0.26, 0.55 nm^2 for Th, MB, CV, respectively (values estimated using the *ChemSketch* 12.01 software).

Alternatively, due to the delocalized π system, the adsorbed cationic dyes can be organised in planar arrangement with the aromatic rings lying flat between the 2D-solid layers. The total area (m^2 g^{-1}) occupied by the adsorbed dyes, A_{dye}, considering these two limit situations (dye molecules adsorbing perpendicular or parallel to the surface), were estimated and are presented in Table 1.

As can be seen from Table 1, and considering a monolayer arrangement, the specific surface area of the NaTNF sample is lower than the area occupied by all the Th and CV molecules (considering both, flat-lying and perpendicular orientations).

Identical conclusion can be taken for the highest MB covering rate (flat-lying orientation), suggesting that at least part of these dyes could be retained within

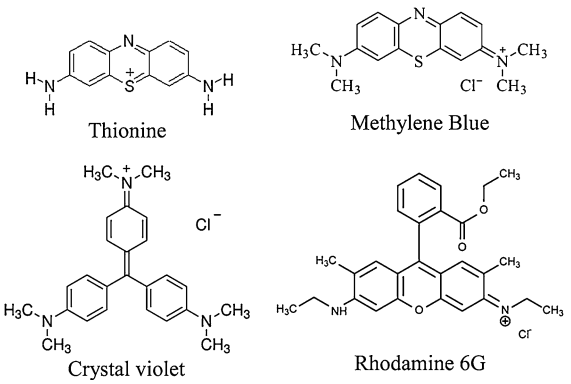

Fig. 3 Molecule schematic representation of the dyes used: thionine (Th), methylene blue (MB), crystal violet (CV) and rhodamine 6G (R6G)

Table 1 BET surface area (A_{BET}), amount (mg g^{-1}) and area occupied by the dyes adsorbed (A_{dye}) in the NaTNF and HTNF surfaces

Sample ID	A_{BET} (m^2 g^{-1})	Dye	Adsorbed dye (mg g^{-1})	A_{dye} (m^2 g^{-1})	
				a*	b*
NaTNF	21.08	Th	126.39	31.78	155.75
		MB	37.68	18.38	60.94
		CV	89.89	72.71	105.61
HTNF	38.90	Th	9.99	2.51	12.31
		MB	9.22	4.50	14.91
		CV	1.74	1.41	2.04

* Total occupied area considering the dye molecule with (a) horizontal and (b) parallel orientation relative to the surface

the NaTNF lamellar structure. The organic dyes intercalation between the TiO_6 layers is feasible for the NaTNF, since this sample possesses sodium ions available to be exchanged in the interlayer space. In fact it has been reported that cationic dyes can be intercalated in the interlayer spacing of layered materials such as clays (Czímerová et al. 2004) and nanostructured titanates (Miyamoto et al. 2004). This also seems to be a reasonable assumption as the dyes molecule dimensions and the TNF's interlayer distance (8.554 Å for the protonated TNFs and 9.403 Å for the NaTNFs) are in agreement with the dye intercalation occurring with the molecules in a parallel position relatively to the TiO_6 layers (Fig S1).

In contrast, the HTNF specific surface area is higher than the one required for accommodating all the dyes molecules adsorbed. This is true even considering the highest surface coverage (perpendicular molecule orientation).

In order to conclude about the formation of new hybrid TNFs materials through these cationic organic molecules intercalation, studies involving XRD, TEM, DRS and FTIR analyses were carried out.

NaTNF hybrid materials structural characterisation

The structural characterisation of the NaTNF samples after dyes sensitization was performed mainly by XRD (Fig. 4).

With Thionine (Th)

The area occupied for the total amount of the immobilized Th (31.78–155.75 $m^2\ g^{-1}$, depending on the molecules configuration) is considerably higher than the NaTNF surface area (21.08 $m^2\ g^{-1}$), indicating that the Th intercalation hypothesis should be carefully analysed.

The size of the thionine dye is 12.54 × 5.32 Å. The thickness of the Th molecule (~2 Å) is smaller than the interlayer distance, d, obtained from the XRD diffraction data for the pristine NaTNF material ($d = 9.403$ Å). On the other hand, literature reports demonstrate that this dye can fit into the main channel of a zeolite, which has an opening of about 7.1 Å (Calzaferri and Cfelkr 1992).

To study the intercalation of the small Th molecules between the TiO_6 layers, and considering a flat and parallel orientation of the molecules in the interlayer space, different amounts of the dye were used in the adsorption experiments. The XRD patterns of different Th-NaTNFs samples are shown in Fig. 4a. A clear shift to higher values in the 2θ peaks, near 10°, was observed. This shift increases with the increase of the dye amount used and agrees with a progressive $Na^+ \rightarrow$ cationic dye exchange process. A shift from 9.4033 to 9.2529 Å was observed in the interlayer distance after saturating NaTNF with Th (sample Th(S)-NaTNF). Additionally, the decrease in these diffraction peaks intensity indicates a partial loss of the structural features due to a reduction of the interlayer distance between the TiO_6 layers. This result can be explained considering the intercalation of the Th molecules.

With Methylene blue (MB)

The amount of MB immobilized using the NaTNF material is higher (1.787 mg m^{-2}) than the one reported for similar TNFs materials (0.844 mg m^{-2}) (Xiong et al. 2010), suggesting the existence of dye intercalation in the NaTNF structure.

The methylene blue molecule can be seen as having a rectangular shape; with dimensions of approximately 14.3 × 6.0 Å and thickness of 1.8 Å (values estimated using the *ChemSketch* 12.01 software). The thickness of the MB molecule is comparable to the one of Th and well-match with the dye intercalation considering a parallel orientation of the MB molecules in relation to the TiO_6 sheets. The XRD patterns of the NaTNF before and after MB saturation are presented in Fig. 4b. A shift to higher values in the 2θ peaks, near 10°, was observed. This shift was 0.134 Å, from 9.4033 Å in the NaTNF to 9.2694 Å in the MB(S)-NaTNF sample (sample with the highest MB content). This result also agrees with a $Na^+ \rightarrow MB^+$ exchange process.

With Crystal violet (CV)

The area occupied by the total amount of CV, the biggest molecule, when in contact with NaTNF (Table 1), and independent on the molecules arrangement, is higher than the available surface area of the pristine material. This suggests dye intercalation within the TiO_6 layers, in a flat and parallel arrangement. The CV molecule thickness (~4 Å), is twice of

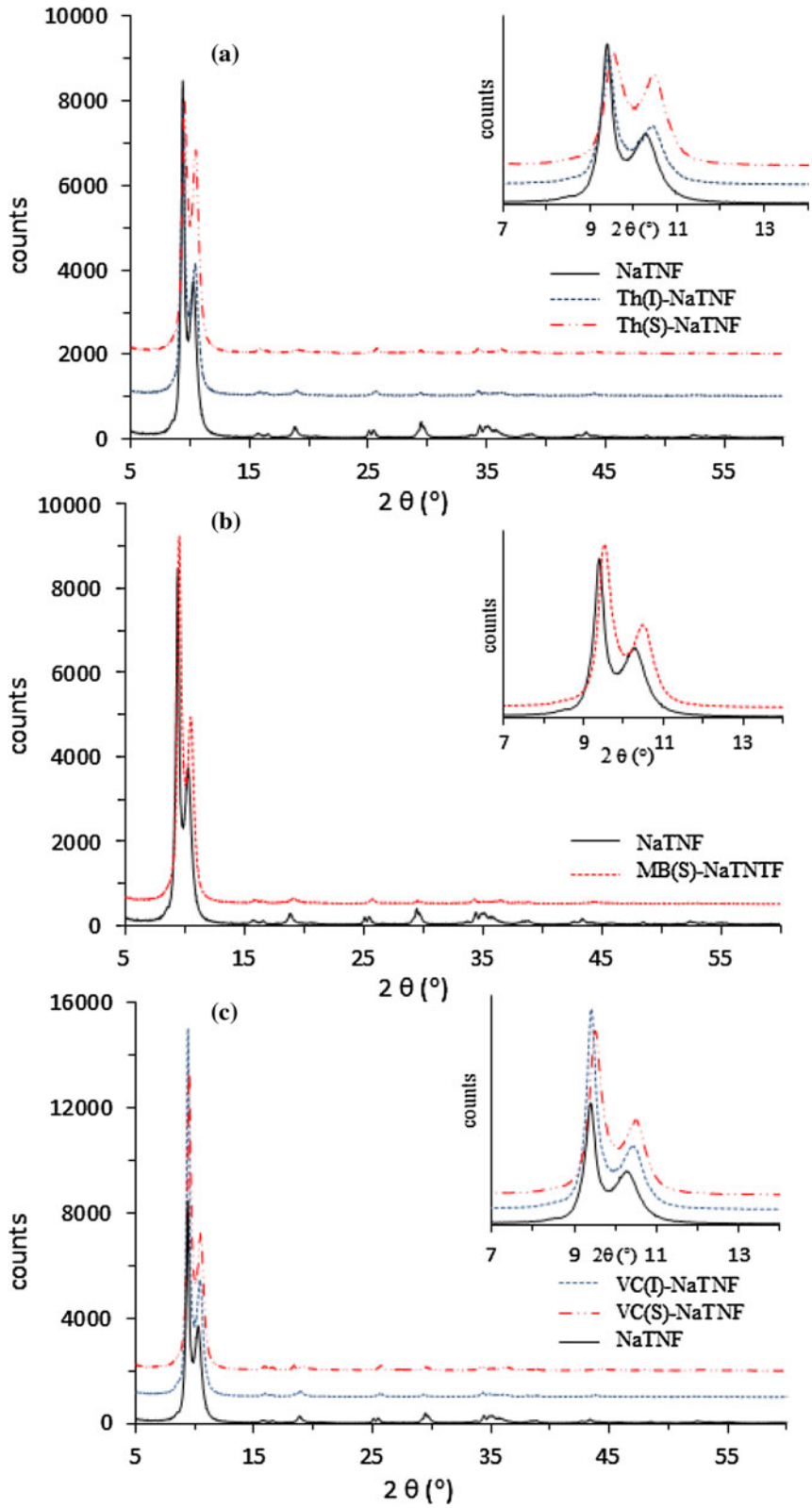

Fig. 4 XRD patterns of the NaTNF sample before and after **a**—Th, **b**—MB and **c**—CV treatment

the Th one. However it is smaller enough to be compatible with the interlayer distance available in the NaTNF structure. The XRD patterns of different CV-NaTNFs, prepared using different amount of this dye, are shown in Fig. 4c. The hybrid CV(S)-NaTNF material, with the highest amount of incorporated CV (dye saturation) presents a structure with an interlayer distance, d, of 9.2859 Å. As in the Th(S)-NaTNF and MB(S)-NaTNF materials, the gradual shift in the $2\theta \sim 10^{\circ}$, with the increase of the amount of immobilized dye, suggests the progressive CV intercalation between the TiO_6 layers.

HTNF hybrid materials structural characterisation

The main difference between the NaTNF and the HTNF samples is the total replacement of the sodium ions by protons and consequent adjustment in the interlayer dimension between the TiO_6 layers, together with some changes in the acidity character of the material. It is reported that the protonation and aggregation of the organic dyes strongly depends on the size and acidity of the nanochannels and/or nanocavities of the hosts (Senthilkumar et al. 2010).

Independent of which dye is being used, the absence of intercalation is predictable for the HTNF sample since its surface area is compatible with the dyes adsorption process alone. Figure 5a shows the HTNF XRD patterns obtained before and after saturation with this dye (sample Th(S)-HTNF). The absence of a shift in the peaks at $\sim 10^{\circ}$ and the preservation of the curve profile suggest the occurrence of dye adsorption only. Conversely, a decrease and broadening in these peaks indicate some modifications, with possible partial loss or reduction of the lamellar structure, after dye treatment. The XRD results obtained for the MB(S)-HTNF sample (Fig. 5b) were similar to the ones obtained for Th(S)-HTNF. The XRD and adsorption results are not conclusive about the possibility of these dyes being intercalated in the HTNF material. But since no 2θ shift was observed, if intercalation occurs it must not imply any changes in the TiO_6 interlayer distance.

On the other hand, distinct results were obtained using CV as intercalating compound. Figure 5c shows the XRD patterns obtained before and after CV saturation and no shift in the peak at $\sim 10^{\circ}$ was observed. However, it is interesting to note that in this material, and contrary to the Th(S)-HTNF and MB(S)-HTNF samples, no changes in the shape and intensity of this peak was visualized. This indicates no changes in the interlayer region, with the protons still between the TiO_6 layers. This suggests no CV intercalation. This result can be explained considering that, from the three studied dyes, the CV molecule is the one with the biggest size.

Hybrid materials characterisation by UV–Vis diffuse reflectance spectroscopy

The optical properties of titanate nanotubes can be modified in a controlled way using ion-exchange reactions. This methodology is suitable for searching modifications in the chemical bonds of the structure, thus, allowing to recognize the titanate nanotubular composition and structure (Xiao et al. 2008). Since UV–Vis spectroscopy is considered a powerful technique for obtaining information about coloured organic–inorganic materials, the prepared materials were studied by diffuse reflectance spectroscopy (DRS). The absorption spectra of the HTNF sample before and after MB and CV saturation (samples MB(S)-HTNF and CV(S)-HTNF, respectively) are presented in Fig. 6. The HTNF band edge absorption (400–300 nm) shifts to higher energies after the dyes immobilization. This blue shift is higher for the MB-HTNF material. The band gap energy increase was from 3.14 eV (HTNF) to 3.32 eV for MB(S)-HTNF and to 3.24 eV for CV(S)-HTNF. The MB(S)-HTNF absorption spectrum profile, in the visible range, is indicative of MB adsorbed in the HTNF surface, in monomeric and polymeric forms (Yan et al. 2005). The presence of a small amount of CV over the HTNF surface can be inferred by the analysis of the CV(S)-HTNF spectrum. After the analysis of the adsorption, XRD and DRS results for these two materials (CV(S)-HTNF and MB(S)-HTNF), it can be concluded that no intercalation occurs in these systems, with the adsorption as the unique process involved in these dyes removal.

The absorption spectra of the NaTNF, Th(S)-NaTNF, MB(S)-NaTNF and CV(S)-NaTNF samples are presented in Fig. 7. For comparative purposes, the aqueous dyes' absorption spectra are also presented. As it can be seen, the absorption spectra of the hybrid materials are similar and practically independent of the dye in use. After combination with the cationic species, a clear decrease in the NaTNF absorption band intensity ($\sim$350 nm) was observed. This indicates a strong modification on the absorption

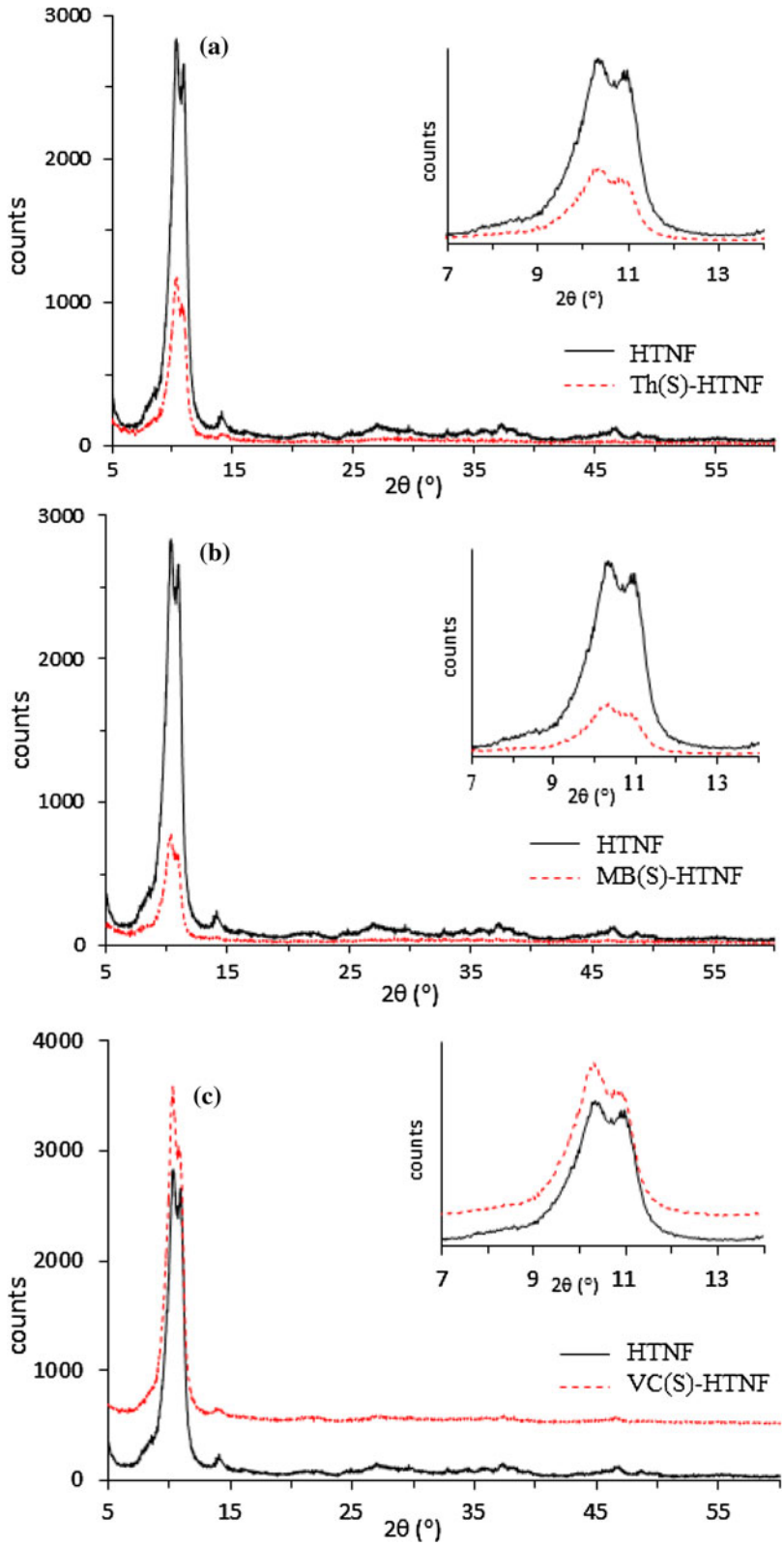

Fig. 5 XRD patterns of the HTNF sample before and after **a**—Th, **b**—MB and **c**—CV treatment

properties of the semiconductor material. The above alterations cannot be completely explained by a surface adsorption process and should be attributed to the dyes intercalation between the TiO_6 layers in the NaTNF elongated structure. The absorption of visible radiation, by these new hybrid materials, can be attributed to the presence of dye aggregates, mainly H-aggregates (Czímerová et al. 2004; Miyamoto et al. 2004). Due to the similarity observed for all the dye-NaTNF absorption profiles, the contribution of these new build hybrid structures in this absorption behaviour cannot be completely ruled out.

The optical behaviour of the Th(S)-NaTNF and Th(S)-HTNF samples are similar (Fig. 7—inset), suggesting the presence of materials with the same structure. That can be explained by the occurrence of dye intercalation in both materials. Comparing these samples, a slight red shift in the 350 nm band edge for the Th(S)-HTNF sample was observed. It is interesting to note that this 350 nm red-shift is identical to the one previously observed for the pristine materials, NaTNF and HTNF (Fig. 2a). Considering these results, the Th intercalation in the HTNF sample can be acknowledged, even in a small scale, since the interlayer distance obtained for the protonated TNFs (8.554 Å) is compatible with the small Th molecules intercalation. Due to its reduced size, the introduction of such species between the TiO_6 layers can occur without changes in the interlayer distance, as predictable by the XRD results.

MB-NaTNF

MB is an organic compound often used to study in detail the adsorption properties of semiconductor nanomaterials (Albuquerque et al. 2008; Bavykin et al. 2010; Xiong et al. 2010, 2011). The sensitization of the NaTNF with MB was analysed in more detail by DRS, in order to contribute to the clarification of the adsorption and intercalation processes rate.

The optical spectra of several MB sensitized TNFs powders, obtained using different MB amounts, are presented in Fig. 8. The optical spectrum of the powder with the lowest MB amount (MB(I)-NaTNF) is similar to the one of the saturated MB(S)-HTNF sample (Fig. 8—inset). It is interesting to notice that these two absorption spectra are similar, mainly in the UV-range. The MB(S)-NaTNF spectrum in the visible range presents a broad peak centred at ~550 nm and a shoulder at 665 nm. These bands, at lower wavelengths than the MB chromophoric peak, are usually associated with the presence of H-aggregates of the dye adsorbed over the matrix surface. The similarity between the MB(I)-NaTNF and MB(S)-HTNF spectra suggests that the adsorption of the dye in the NaTNF surface is the most relevant process in this stage. The formation of dimmers of the dye on the surface of nanofibers can be inferred and could suggest the formation of a multi-layered coating.

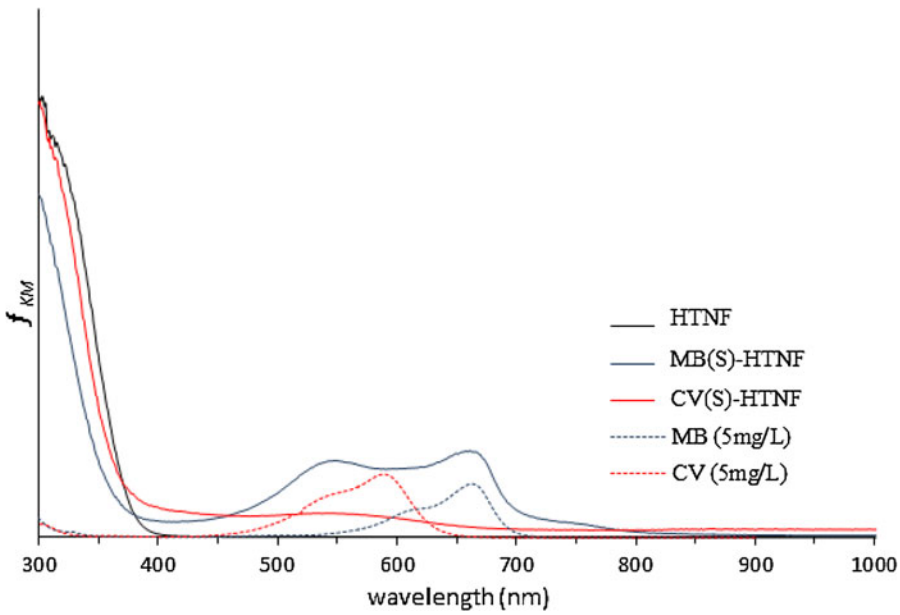

Fig. 6 Absorption spectra of the HTNF, MB(S)-HTNF and CV(S)-HTNF prepared samples. The absorption spectra of a MB and CV aqueous solutions (5 mg L^{-1}) are present for comparative purposes

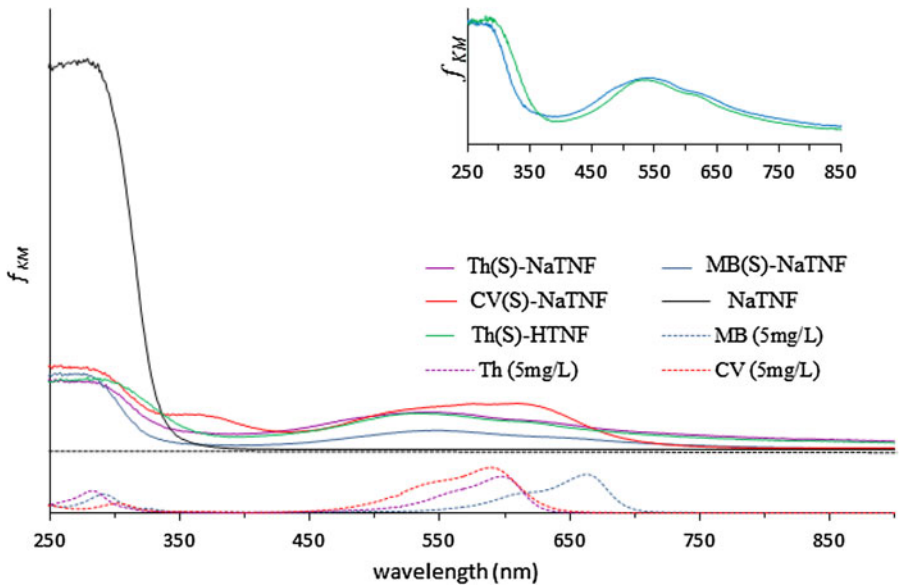

Fig. 7 Absorption spectra of the NaTNF, Th(S)-NaTNF, MB(S)-NaTNF and CV(S)-NaTNF samples. The absorption spectra of a MB and CV aqueous solutions (5 mg L^{-1}) are present for comparative purposes; *inset* Absorption spectra of the Th(S)-NaTNF and Th(S)-HTNF samples

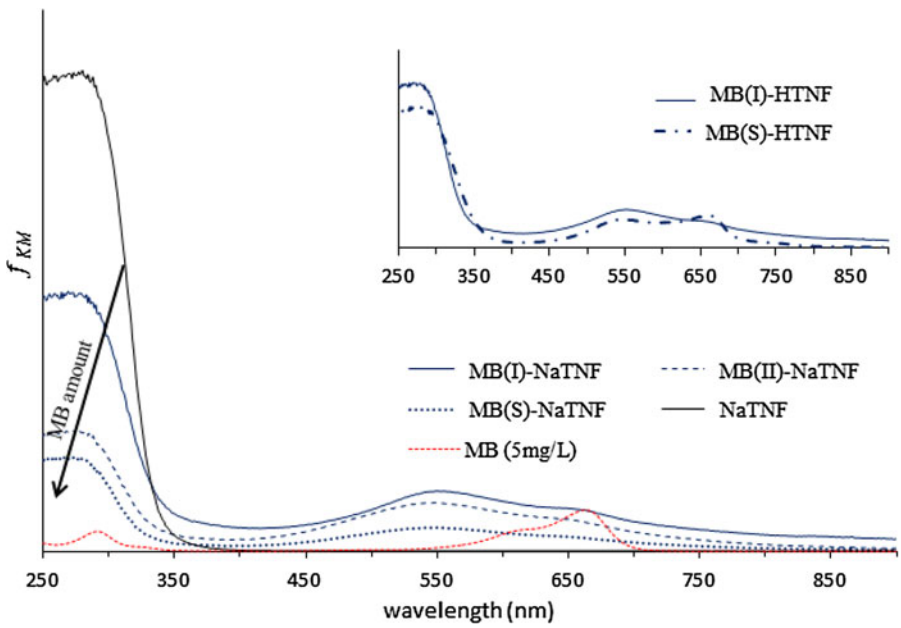

Fig. 8 Absorption spectra of several MB sensitized TNFs powders, obtained using different MB amounts: MB(I) < MB(II) < MB(S); inset: absorption spectra of the MB(I)-NaTNF and MB(S)-HTNF samples

Increasing the amount of dye available in solution, MB(II) and MB(S), an enhancement of the blue-shift and a simultaneous decrease in the characteristic NaTNF and MB absorption bands were observed (Fig. 8). An identical behaviour was observed for the NaTNF samples after gradual sensitization with CV (results not shown). In this stage, these results cannot be explained only by a multi-layered coating formation and suggest, together with the XRD ones, a sequential dye uptake process with a gradual intercalation of the dye between the TiO_6 layers, after an initial surface adsorption stage (sample MB(I)-NaTNF).

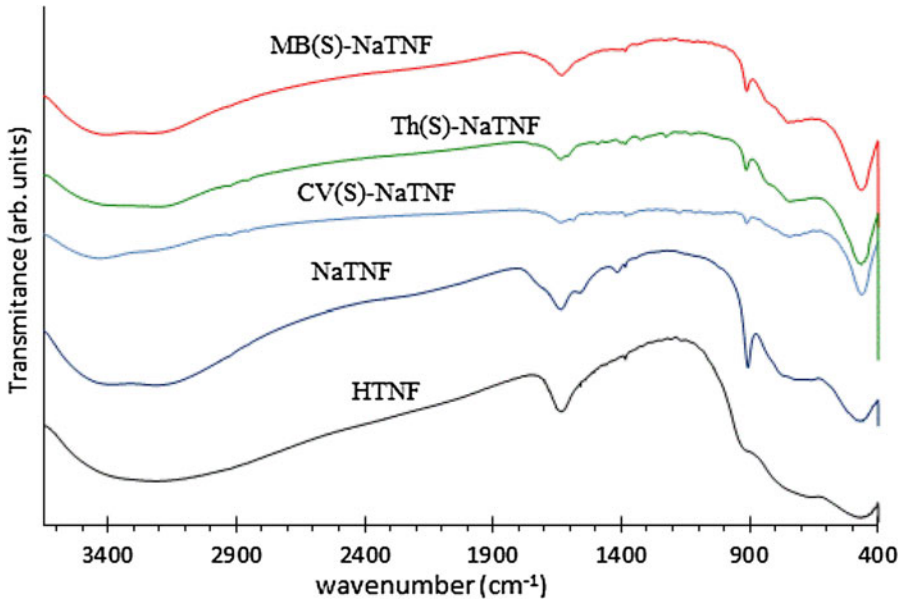

Fig. 9 FTIR spectra of the HTNF, NaTNF, MB(S)-NaTNF, Th(S)-NaTNF and MB(S)-NaTNF samples

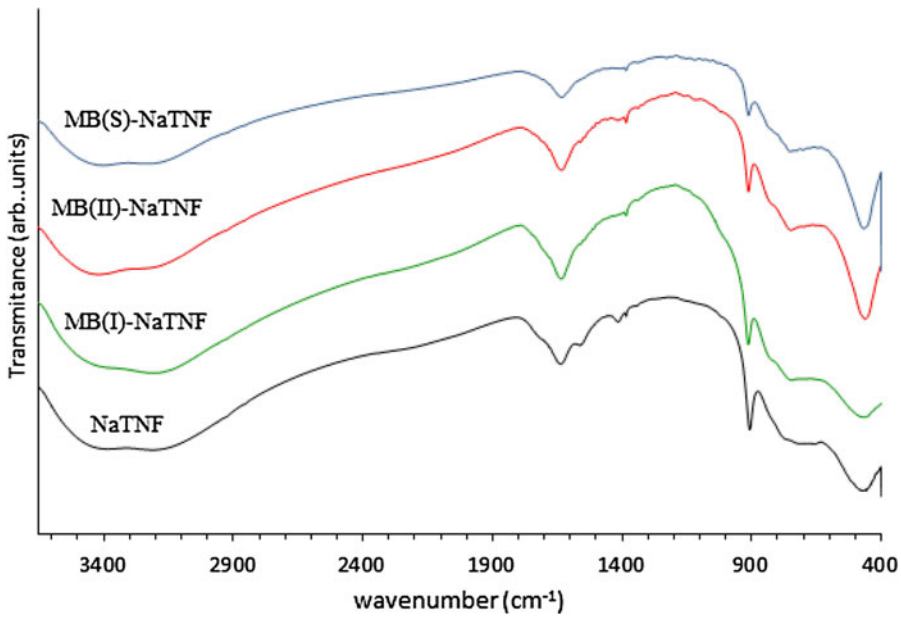

Fig. 10 FTIR spectra of the NaTNF sample before and after MB sensitization; amount of MB immobilized: MB(I) < MB(II) < MB(S)

Hybrid materials characterisation by Fourier transform infrared spectroscopy

To verify the incorporation of the organic dyes molecules within the TiO_6 layers, FTIR was used to characterise the NaTNF and HTNF hybrid materials (Fig. 9). The presence of crystallographic water molecules in the surface of NaTNF (and HTNF) was confirmed by the appearance of the characteristic peak at 1,630 cm^{-1}, that can be assigned to the H–O–H deformation mode (δ_{H-O-H}). The broad intense bands at 3,420 cm^{-1} and 3,180 cm^{-1} can be attributed to surface OH symmetrical and asymmetrical stretching vibrations. A shoulder at 3,180 cm^{-1} from Ti–OH bonds was observed as a consequence of the strong interaction between Ti ions and OH groups within the tubular structure (Bavykin and Walsh 2010). These OH groups' spectra features are less pronounced, or even inexistent, in the HTNF spectrum (Fig. 9), since this sample was submitted to an acid treatment. The wide

band at 463 cm^{-1}, in the NaTNF and HTNF spectra can be assigned to the crystal lattice vibration of TiO_6 octahedra. This band can be affected by the incorporation of ions (via ion-exchange) into the titanate structure, or by the alteration of the elongated morphology. A decrease was observed for the peak at 1,630 cm^{-1} suggesting the release of some water molecules due to the introduction of the dyes in the interlayer space. The NaTNF's broad bands at 3,420 cm^{-1} and 3,180 cm^{-1}, attributed to surface OH groups, decrease after the dyes' treatments. This result indicates the adsorption of dye molecules in the NaTNF surface. A decrease in the band at 914 cm^{-1} and a narrowing of the 463 cm^{-1} bandwidth were observed for all the hybrid dye-NaTNF samples, suggesting an identical uptake process for all the organic molecules. The dyes presence in the samples structure was also confirmed by the appearance of new bands at 1,600–1,100 cm^{-1}. That can be assigned with the aromatic rings of the dyes' molecules and they are present only in the dye-modified NaTNF spectra. No modifications in the FTIR spectra were observed for the HTNF samples, after dyes sensitization (not shown).

For the MB-NaTNF samples (Fig. 10), a narrowing effect in the 463 cm^{-1} band width, related with the vibration of TiO_6 octahedra, is clearly seen with the increase of the MB amount immobilized. The absorption band at 914 cm^{-1} can be assigned to the stretching vibration of short Ti–O bonds, involving non-bridging oxygen coordinated with sodium ions (Dias et al. 2012). A gradual decrease in this band intensity, for the NaTNF modified samples, was observed with the increase of the MB amount uptake. These results are in agreement with a sodium-cationic dye exchange process, with the progressive intercalation of the cationic dye into the NaTNF interlayer space. The TEM images for all the modified NaTNF materials showed the preservation of the elongated morphology in opposition to published works, indicating the total collapse of the tubular morphology after organic acid and bases treatments (Rodrigues et al. 2010).

Conclusions

New titanates nanostructured hybrid materials were easily and successfully prepared through the combination of elongated titanate nanostructures (TNFs) with cationic organic molecules. The intercalation of the organic dyes was dependent on the ion exchange ability of the TNFs and on the organic molecules size and protonation equilibrium constants. The sample with the highest sodium content (NaTNF) was the best dyes up taking material and the intercalation of thionine, methylene blue and crystal violet between the TiO_6 layers was achieved. The characterisation results obtained by adsorption, XRD and FTIR are in agreement with the production of new hybrid structures, where the organic molecules are located amongst the TiO_6 layers. Due to the smaller dimension of the HTNF interlayers, only the thionine molecules demonstrate to have the size required to be incorporated in the structure without changes in the interlayer distance. Using the protonated titanates (HTNF), the removal of the other dyes from solution was only achieved by surface adsorption. The optical characterisation of the prepared materials by DRS agrees with the dyes intercalation and additionally point out the influence of the dyes inserted in the lamellar assembly in the final absorption properties of the prepared hybrid materials.

Acknowledgments This study was supported by Fundação para a Ciência e a Tecnologia (PTDC/CTM NAN/113021/2009). O.C. Monteiro acknowledges PEst-OE/QUI/UI0612/2013 and Programme Ciência 2007.

References

Ackermans B, Schoonheydt RA, Ruiz-Hitzky E (1996) Intercalation of methylene blue into vanadium pentoxide gels. J Chem Soc Faraday Trans 92(22):4479–4484

Albuquerque R, Neves MC, Mendonça MH, Trindade T, Monteiro OC (2008) Adsorption and catalytic properties of SiO_2/Bi_2S_3 nanocomposites on the methylene blue photodecolorization process—colloids and surfaces A: physicochem. Eng Aspects 328:107–113

Bavykin DV, Walsh FC (2007) Kinetics of alkali metal ion exchange into nanotubular and nanofibrous titanates. J Phys Chem C 111:14644–14651

Bavykin DV, Walsh FC (2009) Elongated titanate nanostructures and their applications. Eur J Inorg Chem 997 and references cited therein

Bavykin DV, Walsh FC (2010) Titanate and titania nanotubes: synhtesis, properties and applications—RSC nanoscience & nanothecnology. RSC Publishing, Cambridge

Bavykin DV, Friedrich JM, Walsh FC (2006) Protonated titanates and TiO_2 nanostructured materials: synthesis, properties, and applications. Adv Mater 18:2807–2824

Bavykin DV, Redmond KE, Nias BP, Kulak AN, Walsh FC (2010) The effect of ionic charge on the adsorption of

organic dyes onto titanate nanotubes. Aust J Chem 63: 270–275

Bem V, Neves MC, Nunes MR, Silvestre AJ, Monteiro OC (2012) Influence of the sodium/proton replacement on the structural, morphological and photocatalytic properties of titanate nanotubes. J Photochem Photobiol A 232:50–56

Calzaferri C, Cfelkr N (1992) Thionine in the cage of zeolite L. J Phys Chem 96:3428–3435

Cenens J, Schoonheydt RA (1988) Visible spectroscopy of methylene blue on hectorite, laponite B, and barasym in aqueous suspension. Clay Clay Miner 36:214–224

Cheng W, Shen Y, Wu G, Gu F, Wang JZL (2010) Preparation and properties of a phthalocyanine-sensitized TiO_2 nanotube array for dye-sensitized solar cells. Semicond Sci Technol 25:125014–125018

Cui H, Dwight K, Soled S, Wold A (1995) Surface acidity and photocatalytic activity of Nb_2O_5/TiO_2 photocatalysts. J Solid State Chem 115:187–191

Czímerová A, Jankovič L, Bujdák J (2004) Effect of the exchangeable cations on the spectral properties of methylene blue in clay dispersions. J Coll Interf Sci 274:126–132

Diamandescu L, Vasiliu F, Tarabasanu-Mihaila D, Feder M, Vlaicu AM, Teodorescu CM, Macovei D, Enculescu I, Parvulescu V, Vasile E (2008) Structural and photocatalytic properties of iron- and europium-doped TiO_2 nanoparticles obtained under hydrothermal conditions. Mater Chem Phys 112:146–153

Dias CFB, Araújo-Chaves JC, Mugnol KCU, Trindade FJ, Alves OL, Caires ACF, Brochsztain S, Crespilho FN, Matos JR, Nascimento OR, Nantes IL (2012) Photo-induced electron transfer in supramolecular materials of titania nanostructures and cytochrome c. RSC Advances 2:7417–7426

Kasuga T, Hiramatsu M, Hoson A, Sekino T, Niihara K (1998) Formation of titanium oxide nanotube. Langmuir 14: 3160–3163

Khurana TK, Santiago JG (2009) Effects of carbon dioxide on peak mode isotachophoresis: simultaneous preconcentration and separation. Lab Chip 9:1377–1384

Li X, Liu L, Kang S-Z, Mu J, Li G (2012) Titanate nanotubes co-sensitized with cadmium sulfide nanoparticles and porphyrin zinc. Catal Commun 17:136–139

Luis AM, Neves MC, Mendonca MH, Monteiro OC (2011) Influence of calcination parameters on the TiO_2 photocatalytic properties. Mat Chem Phys 125:20–25

Ma R, Sasaki T, Bando Y (2005) Alkali metal cation intercalation properties of titanate nanotubes. Chem. Commun 948–950

Matsuo Y, Konishi K (2012) Intercalation of various organic molecules into pillared carbon. Carbon 50:2280–2286

Miyamoto KNK, Ogawa M (2004) Visible light induced electron transfer and long-lived charge separated state in cyanine dye/layered titanate intercalation compounds. J Phys Chem B 108:4268–4274

Nunes MR, Monteiro OC, Castro AL, Vasconcelos DA, Silvestre AJ (2008) A new chemical route to synthesise TM-doped (TM = Co, Fe) TiO_2 nanoparticles. Eur J Inorg Chem 28:961–965

Ray M, Chatterjee S, Das T, Bhattacharyya S, Ayyub P, Mazumdar S (2011) Conjugation of cytochrome c with hydrogen titanate nanotubes: novel conformational state with implications for apoptosis. Nanotechnology 22: 415705–415712

Riss A, Berger T, Grothe H, Bernardi J, Diwald O, Knozinger E (2007) Chemical control of photoexcited states in titanate nanostructures. Nano Lett 7:433–438

Rodrigues CM, Ferreira OP, Alves OL (2010) Interaction of sodium titanate nanotubes with organic acids and base: chemical, structural and morphological stabilities. J Braz Chem Soc 21:1341–1348

Senthilkumar K, Paul P, Selvaraju C, Natarajan P (2010) Preparation, characterization, and photophysical study of thiazine dyes within the nanotubes and nanocavities of silicate host: influence of titanium dioxide nanoparticle on the protonation and aggregation of dyes. J Phys Chem C 114:7085–7094

Tchinsoann K, Hester D (1984) Raman spectroscopic studies of a thionine-modified electrode. J Chem Soc Faraday Trans I 80:2053–2071

Viana BC, Ferreira OP, Souza Filho AG, Hidalgo AA, Mendes Filho J, Alves OL (2011) Alkali metal intercalated titanate nanotubes:a vibrational spectroscopy study. Vib Spectrosc 55:183–187

Wong CL, Tan YN, Mohamed A (2011) A review on the formation of titania nanotube photocatalysts by hydrothermal treatment. J Environ Manag 92:1669–1680

Xiao MW, Wang LS, Wu YD, Huang XJ, Dang Z (2008) Electrochemical study of methylene blue/titanate nanotubes nanocomposite and its layer-by-layer assembly multilayer films. J Solid State Electrochem 12:1159–1166

Xiong L, Yang Y, Mai J, Sun W, Zhang C, Wei D, Chen Q, Ni J (2010) Adsorption behavior of methylene blue onto titanate nanotubes. Chem Eng J 156:313–320

Xiong L, Sun W, Yang Y, Chen C, Ni J (2011) Heterogeneous photocatalysis of methylene blue over titanate nanotubes: effect of adsorption. J Colloid Interface Sci 356:211–216

Yan Y, Zhang M, Gong K, Su L, Guo Z, Mao L (2005) Adsorption of methylene blue dye onto carbon nanotubes: a route to an electrochemically functional nanostructure and its layer-by-layer assembled nanocomposite. Chem Mater 17:3457–3463

Ylhainen EK, Nunes MR, Silvestre AJ, Monteiro OC (2012) Titania-free synthesis of titanate nanostructures and their adsorption/photocatalytic properties. J Mater Sci 47:4305–4312

Zhang S, Chen Q, Peng L-M (2005) Structure and formation of $H_2Ti_3O_7$ nanotubes in an alkali environment. Phys Rev B 71:014104–014115